

# IMPACT RESPONSE OF THICK COMPOSITE STRUCTURES

**Niels van Hoorn<sup>1,\*</sup>, Christos Kassapoglou<sup>2</sup>, Wouter van den Brink<sup>1</sup>**

<sup>1</sup> NLR - Netherlands Aerospace Centre, Marknesse, The Netherlands

<sup>2</sup> Faculty of Aerospace Engineering, Delft University of Technology, Delft, The Netherlands

\* niels.van.hoorn@nlr.nl

**Keywords:** Impact, thick composites, impact response

**Summary:** *The impact response, in terms of force and displacement histories, is not yet completely understood for thick composite structures. Hence, the goal of this study is to understand how a thick composite plate behaves under impact, assuming no damage, and how this behaviour differs from that of thin composite plates. The elastic response is studied using an analytical impact response model based on a series expansion and a Hertz contact law and compared to numerical results. Small-mass and large-mass 50J impact events are studied. Generally, a good agreement between the analytical and numerical impact response model is found. A sensitivity analysis shows that the response is especially sensitive to impactor mass and sensitive to laminate dimensions. For small-mass impact the thickness is of paramount influence, in contrast to large-mass impact where the area and aspect ratio significantly determine the response. For thick composite structures less energy is converted into bending and more energy is transformed to indentation.*

## 1. INTRODUCTION

Composite materials are known for their high specific strength properties and, unfortunately, for their low damage tolerance. Especially impact damage (e.g. due to tool drops or hail) can be complex and therefore difficult to predict. To compensate for these uncertainties knock-down factors are used which drive the weight and cost of the structure. Accurate damage models might be able to quantify the damage tolerance and result in a better understanding of the damage mechanisms. In turn these models could aid the design and certification process and give a better indication of optimal knock-down factors for impact damage.

Thick composite structures (i.e. 20-50mm or 80-200 layers) are used in highly loaded aerospace structures, such as lugs or landing gear components. For these structures the impact response and damage mechanisms are not completely understood. This paper studies the impact response of a square plate, in terms of force and displacement histories, assuming no damage. Beside the response as a function time, the force versus impactor displacement is a useful way of interpreting the response. This study is part of a an on-going research program on impact damage tolerance of thick composite structures and its goal is to understand the impact response and the differences with impact on thin composite structures before modelling the complex damage mechanisms.

Analytical models that predict the response are available. Some authors that have contributed in this field are Shivakumar [1], Christoforou [2, 3], Olsson [4, 5] and more recently Talagani [6]. The methods they use include energy-balance models to predict the peak force [7], simple spring-mass models that determine the response over time, and more complex models involving series expansions. The spring-mass models can result in efficient closed-form solutions, while the energy-balance models generally require an iterative approach and while more complex models, involving non-linear differential equations, which requires numerical solution techniques. In addition, all these models need a contact formulation that describes the interaction between the impactor and the laminate. The most popular formulation is the Hertz contact law [8], that is frequently used in analytical response models. On the other hand the model of Christoforou and Yigit [9] is very accurate for elasto-plastic contact. Talagani studied several contact formulations in his PhD thesis [6] for different phases, elastic loading, elasto-plastic loading, unloading, and reloading. In this paper one of these analytical response models is selected and modified to study the impact response on a thick composite plate.

The contact formulation is given in Section 2, followed by the analytical and numerical impact response models in Section 3, which are compared in Section 4.1. Subsequently a sensitivity analysis is performed using the analytical impact response model of which the results are given in Section 4.2. A summary and conclusions are given in Section 5.

## 2. CONTACT FORMULATION

This study uses the Hertz contact law, as given in Equation 1. The Hertz contact law is only accurate in case the indentation ( $\delta$ ) is smaller than the impactor and laminate dimensions [4, 6]. However, in Section 4 it is found that for impact on thick composite plates there is significantly more indentation due to the lack of plate bending. This was also concluded by Talagani [6], who performed an extensive contact study. For the analytical impact response model in Section 3.1 the Hertz contact law is considered sufficient because it is assumed that no damage occurs.

$$F = k_\alpha \delta^{3/2} \quad (1)$$

$$k_\alpha = \frac{4E_z \sqrt{R_i}}{3(1 - \nu_{rz}\nu_{zr})} \quad (2)$$

For the contact stiffness ( $k_\alpha$ ) in Equation 2 it is assumed that the impactor stiffness ( $E_i$ ) is much larger than the laminate stiffness ( $E_z$ ), such that the impactor with radius  $R_i$  can be modelled as rigid. In Equation 2  $E_z$ , and the Poisson's ratios  $\nu_{rz}$  and  $\nu_{zr}$  are derived from the laminate stiffness tensor ( $\mathbf{C}$ ). The laminate stiffness tensor is obtained by rotating the ply stiffness tensor to the laminate coordinate system and subsequently averaging all the plies. For a layup that is not transversely isotropic  $\nu_{xz} \neq \nu_{yz}$  and therefore  $\nu_{rz}$  is determined by averaging the two. In contrast to the contributions of Olsson [4] and Christoforou [3], this is a more accurate description. In their papers it is assumed that  $E_z \approx E_{22}$  and that  $\nu_{zr} \approx 0$ , which are both not the case (see Table 1(a) and 1(b)). Olsson also mentions that Henriksson [10] did a theoretical and experimental study and found that  $E_z \approx 1.25E_{22}$  [4]. For the material and layup used in this paper a factor of 1.23 is found, i.e.  $E_z = 1.23E_{22}$ .

### 3. IMPACT RESPONSE MODEL

This section presents an analytical and a numerical impact response model. These models predict the impact response of the laminate and impactor in terms of force, displacements and velocity histories. For this study an anti-symmetric balanced transversely isotropic layup is chosen in order to comply with the assumptions in the governing equations. For this layup the B-matrix is zero, as well as the shearing-stretching coupling terms ( $A_{16} = A_{26} = 0$ ) and bending-twisting coupling terms ( $D_{16} = D_{26} = 0$ ).

$$[-45, 45, 0, 90, 45, -45, 90, 0, 0, 90, 45, -45, 90, 0, -45, 45]_n$$

A fabric material with an approximate 85/15 fibre distribution is used with properties as given in Table 1(a) and the equivalent laminate membrane properties of the above layup are given in Table 1(b). Using the contact formulation of Section 2  $k_\alpha$  is calculated to be  $3.48 \text{ GPa}\sqrt{m}$ . According to the assumption of Olsson and Christoforou (i.e.  $E_z \approx E_{22}$  and  $\nu_{zr} \approx 0$ ) the contact stiffness would be  $2.67 \text{ GPa}\sqrt{m}$ , which is a reduction of 23%. This is equivalent to reducing the impactor radius by a factor two of which the effect will be discussed in Section 4.2. The contact stiffness and equivalent laminate membrane properties in Table 1(b) do not depend on the value of  $n$ , but the bending properties (e.g. D-matrix) increase with approximately  $h^3$ . The reference properties used throughout this paper refer to the properties in Table 1 with  $n = 5$  (or  $h = 20\text{mm}$ ).

Table 1. The reference properties: (a) the ply properties (85/15 fabric), (b) the equivalent single layer membrane properties, and (c) additional properties related to the laminate or impactor.

(a)			(b)			(c)		
$E_{11}$	120	GPa	$E_x$	50.52	GPa	$k_\alpha$	3.48	$\text{GPa}\sqrt{m}$
$E_{22}$	20	GPa	$E_y$	50.52	GPa	$a$	0.2	m
$E_{33}$	20	GPa	$E_z$	24.68	GPa	$b$	0.2	m
$G_{12}$	5	GPa	$G_{xy}$	18.78	GPa	$\rho$	1560	$\text{kg/m}^3$
$G_{13}$	5	GPa	$G_{xz}$	4.5	GPa	$R_i$	10	mm
$G_{23}$	4	GPa	$G_{yz}$	4.5	GPa	$E_i$	50	J
$\nu_{12}$	0.3	-	$\nu_{xy}$	0.34	-	$m_{i,small}$	0.04	kg
$\nu_{13}$	0.3	-	$\nu_{xz}$	0.34	-	$m_{i,large}$	4	kg
$\nu_{23}$	0.54	-	$\nu_{yz}$	0.34	-	$v_{i,small}$	50	m/s
$t_{ply}$	0.25	mm	$h$	4·n	mm	$v_{i,large}$	5	m/s

Two types of 50J impact cases are studied, a small-mass 0.04kg (50m/s) impact case (e.g. runway debris) and a large-mass 4kg (5m/s) impact case (e.g. tool drop). In the subsequent sections the reference to small-mass and large-mass impact involves these two cases.

### 3.1 Analytical Model

The impact response model that is used is based on the model of Christoforou [3]. He assumed that the plate center deflection  $w_p$  is described by a series expansion of a modal function. Here  $q_{mn}$  is the unknown amplitude and  $s_{mn}$  for centrally loaded plates is given in Equation 4.

$$w_p = \sum_{m=1}^{\infty} \sum_{n=1}^{\infty} q_{mn} s_{mn} \quad (3) \quad s_{mn} = \sin \frac{m\pi}{2} \sin \frac{n\pi}{2} \quad (4)$$

Inserting Equation 3 into the governing equations gives a set of  $m \times n + 1$  ordinary differential equations describing the plate and impactor behaviour in the equations below, with the initial conditions  $q_{mn}(0) = 0$ ,  $\dot{q}_{mn}(0) = 0$ ,  $\delta(0) = 0$ , and  $\dot{\delta}(0) = v_i$ . Here force ( $F$ ) is described by Equation 2,  $m_p$  is the plate mass and  $v_i$  is the impactor velocity. The natural frequencies of a simply supported composite laminate ( $\omega_{mn}^2$ ) are determined using the Classical Laminated Plate Theory, see Equation 7 [6].

$$\frac{d^2 q_{mn}}{dt^2} + \omega_{mn}^2 q_{mn} = \frac{4F}{m_p} s_{mn} \quad (5) \quad \sum_{m=1}^{\infty} \sum_{n=1}^{\infty} \left( \frac{d^2 q_{mn}}{dt^2} s_{mn} \right) + \frac{d^2 \delta}{dt^2} = -\frac{F}{m_i} \quad (6)$$

$$\omega_{mn}^2 = \frac{1}{h\rho} \left[ D_{11} \left( \frac{m\pi}{a} \right)^4 + 2(D_{12} + 2D_{66}) \left( \frac{m\pi}{a} \right)^2 \left( \frac{n\pi}{b} \right)^2 + D_{22} \left( \frac{n\pi}{b} \right)^4 \right] \quad (7)$$

Equation 6 describes the motion of the impactor by Newton's Second Law  $m_i \ddot{w}_i = -F$ . Here the relation describing the indentation, i.e. difference in the impactor displacement ( $w_i$ ) and the plate center deflection ( $\delta = w_i - w_p$ ), is inserted together with Equation 3.

The system is reduced to the first order by introducing the set of variables in Equation 8. Substituting these variables and the Hertz contact law in Equations 5 and 6 gives the  $2 \times m \times n + 2$  set of first-order ordinary differential equations in Equation 9, with the corresponding initial conditions in Equation 10.

$$\begin{aligned} q_{mn,1} &= q_{mn} & q'_{mn,1} &= q_{mn,2} & q_{mn,1}(0) &= 0 \\ q_{mn,2} &= q'_{mn} & q'_{mn,1} &= \frac{4k_\alpha}{m_p} s_{mn} \delta_1^q - \omega_{mn}^2 q_{mn,1} & q_{mn,2}(0) &= 0 \\ \delta_1 &= \delta & \delta'_1 &= \delta_2 & \delta_1(0) &= 0 \\ \delta_2 &= \delta' & \delta'_2 &= -\frac{k_\alpha}{m_i} \delta_1^q - \sum_{m=1}^{\infty} \sum_{n=1}^{\infty} s_{mn} q'_{mn,2} & \delta_2(0) &= v_i \end{aligned} \quad (8) \quad (9) \quad (10)$$

The system of first order differential equations described above can now be solved using *ode45* within Matlab, which is a function based on a variable step Runge-Kutta method. This outputs the indentation ( $\delta$ ) and, using the Hertz contact law, the force as a function of time. The plate deflection ( $w_p$ ) as a function of time is determined by Equation 3 and the impactor displacement by  $\delta = w_i - w_p$ .

In Figure 1 the solution is verified by comparing it to the results obtained by Christoforou [3]. The first peak is in good agreement, but there is a discrepancy in the second peak. This is probably due to small differences in the numerical solution procedure and the determination of the plate natural frequencies. Only the first peak is of interest for this study and therefore the solution from this method is considered verified.

The model is validated by comparing the solution with 5J impact experiments on a thin composite plate performed by Lopes [11] and the response model of Talagani [6] in Figure 2. The validation is limited because it considers a low energy impact on a thin laminate, which is outside the scope of this study. The result is, beside a shift in the influence of the plate natural frequency, in agreement with the model of Talagani and in line with the experiments of Lopes.

Convergence is checked by increasing the number of  $m, n$  terms in Equation 9. It is observed that for both small-mass and large-mass impact convergence is achieved with 15 terms.

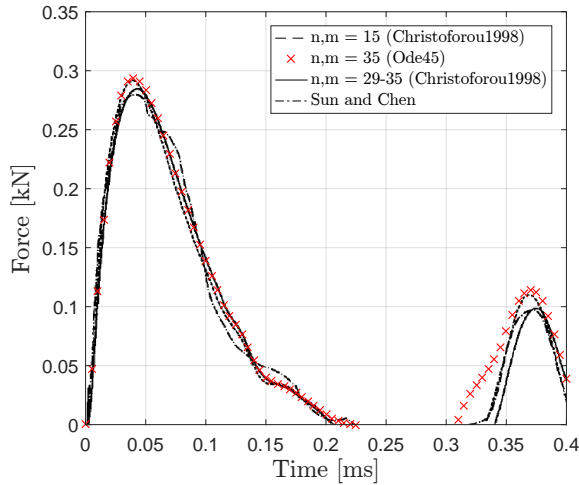


Figure 1. Verification of the analytical impact response model by comparison with Christoforou's solution [3].

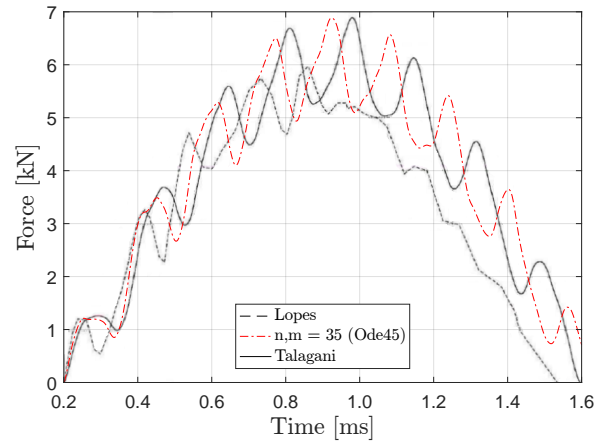


Figure 2. Validation of the analytical impact response model by comparison with impact experiments performed by Lopes [11, 6].

The nature of the response is depends on the involvement of the area affected by flexural waves up to the end of impact ( $t_{imp}$ ). The end of impact, or impact duration, is defined as the moment when the impactor is back at zero displacement. This wave affected area can be determined from the wave front of the first mode, which is described in terms of an ellipse with  $r(\theta)$  as in Equation 11 [5, 12]. Here  $D_r(0^\circ) = D_{11}$  and  $D_r(90^\circ) = D_{22}$  which are the only two values required to define the wave affected area in terms of an ellipse.

$$r(\theta) = \sqrt{\pi t_{imp}} \left[ \frac{D_r(\theta)}{h\rho} \left( \frac{D_{12} + 2D_{33}}{\sqrt{D_{11}D_{22}}} + 1 \right) \right]^{1/4} \quad (11)$$

### 3.2 Numerical Model

In parallel with the analytical model a numerical model is developed. ABAQUS/Explicit is chosen because the impact times are relatively short, i.e. in the order of 0.1ms for small-mass impact and 1ms for large-mass impact. During the development of this model different modelling options are considered and weighted in terms of computational time and accuracy.

As a start a layer-by-layer model with continuum solid elements (C3D8R) is created. For this model the ply properties in Table 1(a) and the corresponding orientations are assigned to each ply and all the plies are tied together using a tie constraint. Hard frictionless contact is defined and the mesh is refined near the contact region. Quarter symmetry is applied and it is observed that this does not affect the response in terms of force and displacement. However, the internal stress distribution is affected due to the symmetry because  $E_{11} \neq E_{22}$ , which will give inaccurate damage predictions.

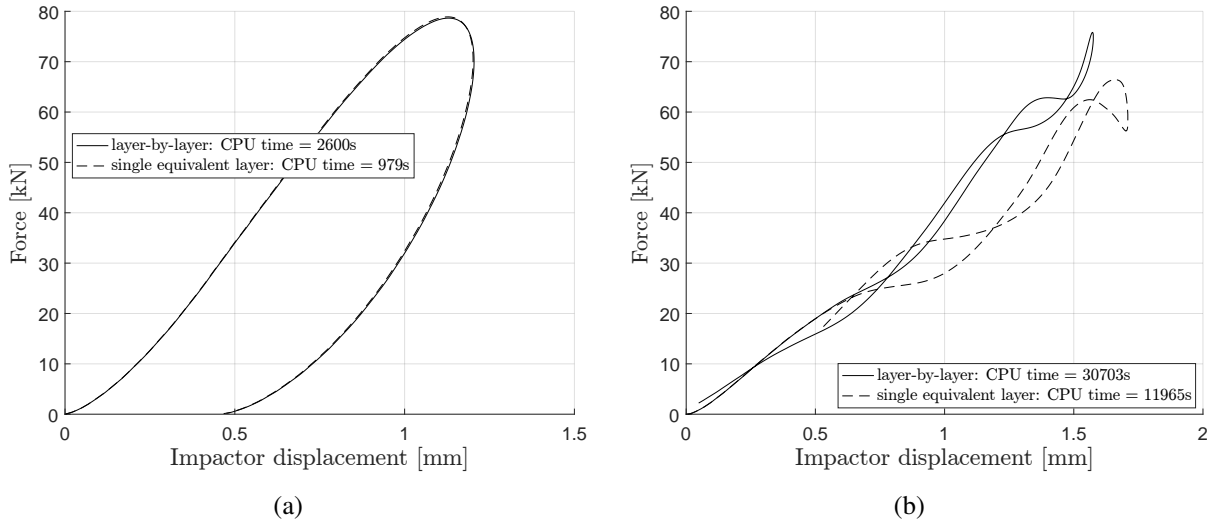


Figure 3. Comparison of the layer-by-layer and single equivalent layer numerical impact response model for (a) small-mass and (b) large-mass impact.

The laminate can also be modelled as a single equivalent layer using the laminate properties given in Table 1(b). The difference between the layer-by-layer and single equivalent layer model is exemplified in Figure 3. For the small-mass impact the results are exactly equal, but for the large-mass impact there is some deviation. The longer impact duration of the large-mass impact event allows the oscillations of the plate to affect the response, resulting in force oscillations. Therefore the natural frequency of the laminate has a significant influence on the result, in contrast to the case of a localised small-mass impact. A change in the properties of the top layer does not affect the contact definition, but representing the laminate as a single equivalent layer with equivalent properties influences the laminate response. In the end the reduction in computational time by more than 60% is considered more important, hence the single equivalent layer model is used.

Several meshing strategies are investigated, for instance a uniform or refined mesh. In the case of the refined mesh the mesh density at the impact location is equal to a uniform mesh, i.e. one element through the thickness, but the mesh density decreases towards the plate edges. There is no noticeable difference in response except for a 92% decrease in computational time for the refined mesh. The convergence of the mesh size is also studied, which is expressed in terms of elements through the thickness ( $n_t$ ). The results converge for  $n_t = 40$ , which is equal to one element for each two plies (0.5mm) and results in an additional 80% decrease in computational time compared to  $n_t = 80$ . Finally, the area of the square refined region is increased from  $1 \times 1$  to  $3 \times 3$  and  $5 \times 5$ mm. The results for both small-mass and large-mass impact converged at a refined region of  $3 \times 3$ mm.

Another popular element for composite laminate simulations is the continuum shell element (SC8R), which has a shell like response but a continuum topology. By comparing these two element types it is concluded that the continuum shell elements have problems with the localised indentation due to a limited through-thickness description compared to the continuum solid elements. Also, a 40% increase in computational time is observed for a small-mass impact case. Due to the above it is concluded that continuum shell elements are not suitable for localised impact cases where large indentations are involved.

#### 4. RESULTS AND OBSERVATIONS

In Section 4.1 the numerical and analytical model are compared. This comparison is a bit arbitrary because in the ideal case both models should be compared to experimental data. However, Figure 2 shows that the analytical model is reasonably close to experimental results. At this point no damage is included in both the analytical and numerical model and therefore it makes sense to compare the analytical and numerical models. In addition to the analytical model based on Christoforou, the small-mass impact model of Olsson [4] and energy-balance model of Esrail [7] are included in the comparison.

##### 4.1 Comparison of Impact Response Models

Figure 4(a) shows the comparison for the small-mass impact event. The analytical impact response model and Olsson's model yield exactly the same results but show some deviation from the numerical model. This is due to the localised behaviour that is not correctly captured by either the analytical or numerical model. The energy-balance model of Esrail was intended for low-velocity impact and therefore quite far off compared to the other models for a 50m/s impact event. For the large-mass impact event in Figure 4(b) the analytical and numerical impact response model, as well as the energy-balance model of Esrail give similar results. Olsson's model is based on a single mass spring and therefore not suitable to capture the influence of plate oscillations. For the case in Figure 4(b) the force oscillations between the analytical and numerical impact response model do not match because it is a difficult dynamic phenomenon to capture correctly. For other cases an exact match was observed, but note here that the single equivalent layer description of the numerical model also plays a role, see Figure 3(b).

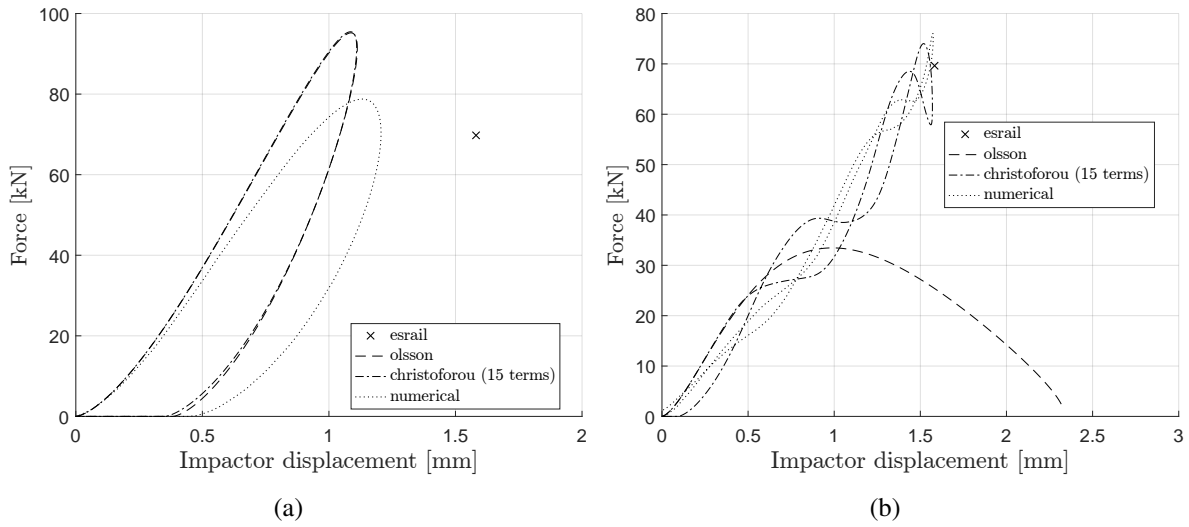


Figure 4. Comparison of the analytical impact response model discussed in Section 2, Olsson’s small-mass impact response model, Esrail’s energy-balance model and the numerical impact response model given in Section 3 for (a) small-mass and (b) large-mass impact.

## 4.2 Sensitivity Analysis

The analytical impact response model is now used to perform a sensitivity analysis. In each case a small-mass and large-mass impact event is studied, except for the sensitivity of impactor mass. The key parameters below that determine the response are varied independently compared to the reference properties in bold.

- Impactor mass ( $m_i$ ):            **0.04** - 0.4 - **4**    kg    (constant  $E_i$ )
- Impactor energy ( $E_i$ ):           **50** - 128 - 200   J    (constant  $m_i$ )
- Impactor radius ( $R_i$ ):           5 - **10** - 20    mm
- Laminate thickness ( $h$ ):        12 - **20** - 40    mm
- Laminate area ( $a, b$ ):           100 - **200** - 400   mm
- Laminate aspect ratio ( $AR$ ):   **1** - 2 - 4            (constant area)

It is observed that the sensitivity to the impactor mass is high and it can significantly change the impact response, see Figure 5. In addition to the increase in impactor duration, from approximately 0.065ms to 0.35ms and to 0.98ms, the response changes from local (small-mass) to quasi-static (large-mass). In between a typical case of an intermediate-mass impact is shown. The three separate types of impact, i.e. small-mass, intermediate-mass, and large-mass impact can be exemplified by looking at the force and plate deflection versus normalised time, as in Figure 6 for a small-mass and large-mass impact. In contrast to a large-mass impact, the force and plate deflection are out of phase for a small-mass impact. For the intermediate-mass impact the force and plate deflection are still out of phase, but the force history is complex as it can increase and decrease significantly over time simulating multiple impacts, see also Figure 5.

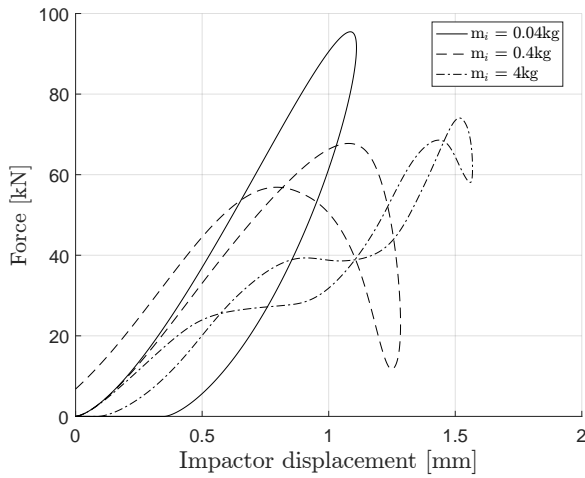


Figure 5. Impactor mass sensitivity.

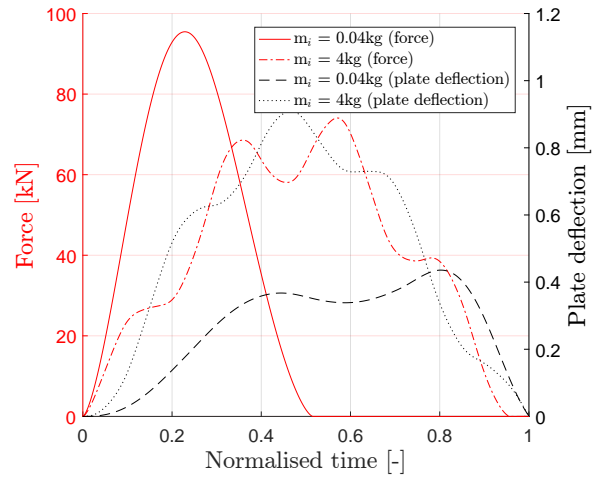


Figure 6. Force and plate deflection for small-mass and large-mass impact.

The transition between the response types also involves the wave affected area as discussed in Section 3 and determined by Equation 11. By calculating the impact time  $t_{imp}$ , it is determined that it takes 0.064ms for the flexural waves to reach the boundaries of the specimen. The impact duration of the small-mass impact case is 0.075ms and it can be seen from Figure 6 that around the time the force is zero at the end of impact the plate oscillations start to occur, which in this case do not affect the response. On the other hand, for the large-mass impact the plate oscillations are visible but the impact duration is too long to significantly affect the response. For an intermediate-mass impact the plate oscillations will significantly affect the response.

The sensitivity to the impactor energy ( $E_i$ ), i.e. the impactor velocity ( $v_i$ ) for a constant impactor mass, is low. However, the force and displacements are increased with approximately the impactor velocity while the impact duration is only slightly decreased. This is expected as the velocity is only an initial condition and can be seen as the amplitude of the system of differential equations. Similar the sensitivity to the impactor radius ( $R_i$ ) has no significant effect on the response shape, but increasing the impactor radius decreases the force and increases the impactor displacement. This effect is similar to scaling the contact stiffness ( $k_a$ ).

The parameters that have a high sensitivity are the laminate dimensions, i.e. the thickness (Figure 7), the area (Figure 8), and the aspect ratio (Figure 9). Increasing the thickness as well as the area doubles the laminate mass and according to Olsson the impactor/plate mass ratio dictates the response [5]. He states that a ratio below 0.23 can be considered small-mass, and above 2.0 large-mass impact. However, it is observed that the sensitivity to these parameters is different. This indicates that the laminate bending stiffness plays a significant role, i.e. increasing the thickness increases the bending stiffness, but increasing the area decreases the bending stiffness. Overall, the area within the force-displacement curve decreases for an increasing thickness. For thicker laminates more energy is absorbed into indentation instead of bending energy during the loading phase. For example, according to the model of Esrail [7], for a thickness of 12mm

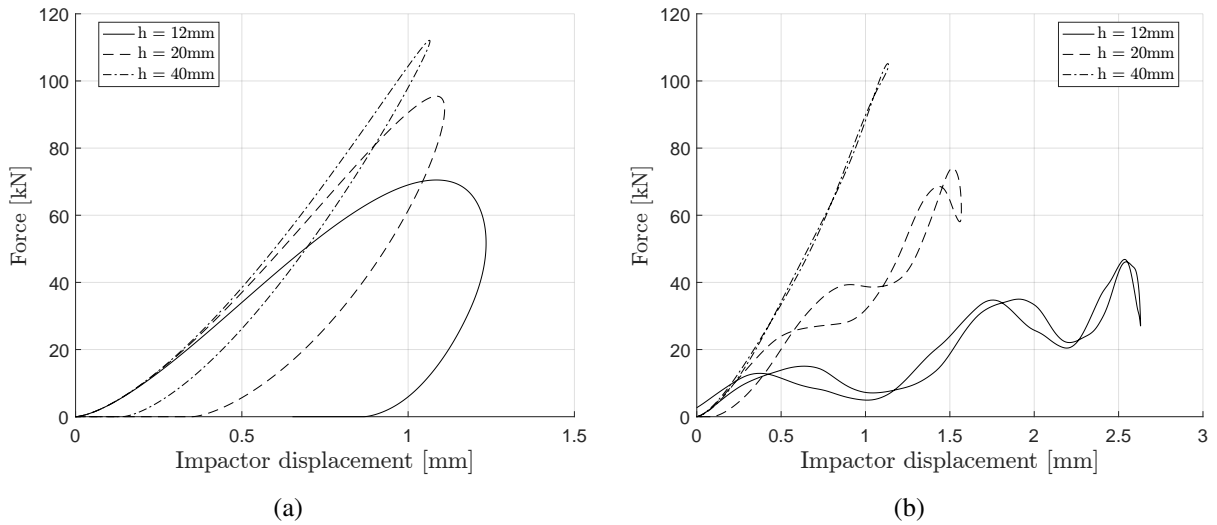


Figure 7. Laminate thickness sensitivity for (a) small-mass and (b) large-mass impact.

about 80% is converted to bending energy compared to 15% for a 40mm thick laminate. Also, for small-mass impact more energy converted back to kinetic energy and therefore the residual velocity is closer to the initial velocity for thicker laminates. For large-mass impact all energy is converted back to kinetic energy resulting in a residual velocity equal to the initial velocity.

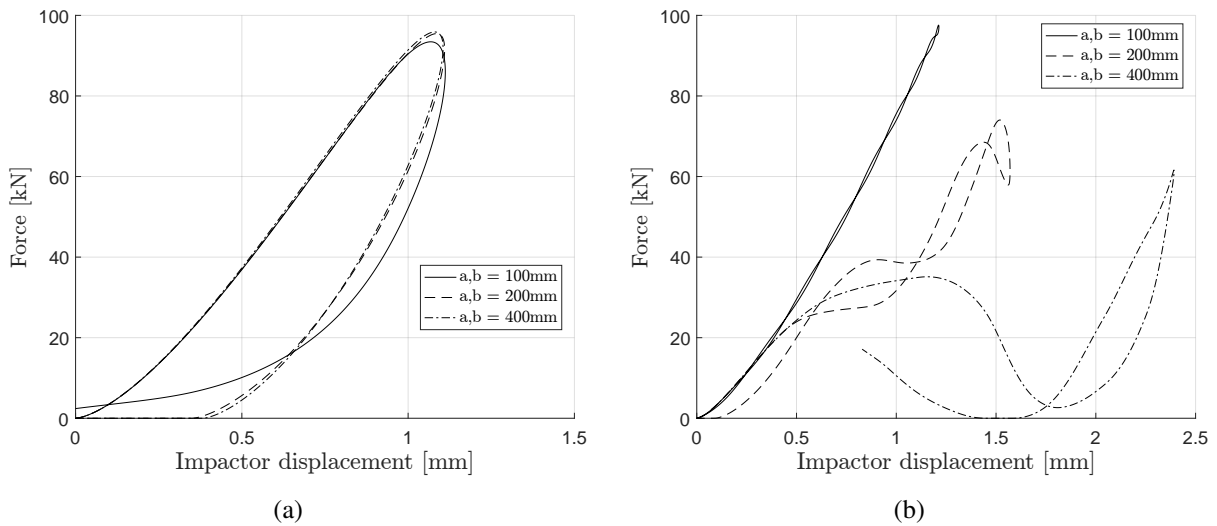


Figure 8. Laminate area sensitivity for (a) small-mass and (b) large-mass impact.

In contrast to large-mass impact, increasing the laminate area above  $200 \times 200\text{mm}$  has no effect on the response for small-mass impact, see Figure 8. The same is observed for the sensitivity to the laminate aspect ratio in Figure 9. It is therefore concluded that in contrast to a localised small-mass impact, large-mass impact is influenced by laminate dimensions and boundary conditions, which is in line with Olsson's conclusions [5].

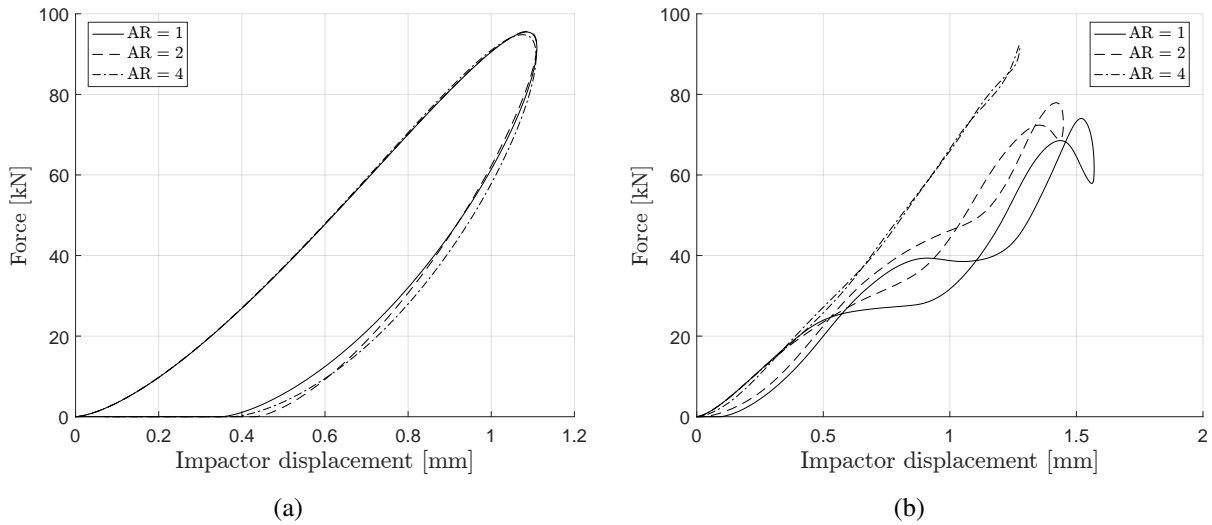


Figure 9. Laminate aspect ratio sensitivity for (a) small-mass and (b) large-mass impact.

## 5. CONCLUSIONS AND FUTURE WORK

The goal of this study was to understand the impact response of thick composite structures and to identify the differences with impact on thin composite structures before modelling complex damage mechanisms. In an effort to do so an analytical impact response model was developed based on the methodology of Christoforou and Yigit [3] and using the Hertz contact law. A numerical impact response model was also developed for comparison and overall a good agreement between both models was observed. Subsequently a sensitivity analysis on several key parameters was performed, using the analytical impact response model for 50J small-mass and large-mass impact events. This leads to the following conclusions:

A small-mass impact results in a localised response where the force and plate deflection histories are out of phase, in contrast to a quasi-static response due to a large-mass impact. For intermediate-mass impacts a complex response is observed. By increasing the impactor velocity, while keeping the impactor mass constant, the force and displacement are increased by approximately the increase in velocity. For a large impactor radius the contact stiffness is higher and thus a higher force and lower indentation are obtained. For large-mass impact the boundaries and thus laminate dimensions play a significant role. Increasing the laminate thickness increases the bending stiffness of the laminate and, therefore, less energy is absorbed in bending and more in indentation. Similarly as for the thickness, decreasing the laminate area results in less bending, but only for large-mass impact. In addition, the response in terms of plate oscillations can be significantly different. Increasing the aspect ratio, while keeping the laminate area constant, has a similar effect as increasing the laminate area. Again, only for large-mass impact.

The response of thick composite structures can be completely different from the response of thin composite structures. For large-mass impact also the laminate area and aspect ratio that

define the boundary play a significant role. In general it can be stated that thicker laminates have a higher bending stiffness and therefore less impact energy is converted to bending and more is converted to indentation. In the end, the energy that goes into bending and indentation will result in damage. Thick composite structures generally have a localised impact response which will have a significant effect on the damage that occurs. From literature and previous studies it is known that the damage is mostly internal in the form of matrix cracking and delaminations and maybe a dent at the impact location. As part of an on-going research project, the goal is to predict this damage and identify the differences with impact on thin composite structures.

## References

- [1] K.N. Shivakumar, W. Elber, and W. Illg. Prediction of impact force and duration due to low-velocity impact on circular composite laminates. *Journal of Applied Mechanics*, 52(3):674–680, September 1985.
- [2] A.P. Christoforou and S.R. Swanson. Analysis of impact response in composite plates. *International Journal of Solids and Structures*, 27(2):161–170, 1991.
- [3] A.P. Christoforou and A.S. Yigit. Characterization of impact in composite plates. *Composite Structures*, 43:14–24, 1998.
- [4] R. Olsson. Impact response of orthotropic composite plates predicted from a one-parameter differential equation. *AIAA Journal*, 30(6):1587–1596, June 1992.
- [5] R. Olsson. Mass criterion for wave controlled impact response of composite plates. *Composites Part A: Applied Science and Manufacturing*, 31(8):879–887, August 2000.
- [6] M.R. Talagani. *Impact analysis of composite structures*. Phd thesis, Delft University of Technology, December 2014.
- [7] F. Esrail and C. Kassapoglou. An efficient approach for damage quantification in quasi-isotropic composite laminates under low speed impact. *Composites Part B: Engineering*, 61:116–126, May 2014.
- [8] H. Hertz and P.E.A. Lenard. *Gesammelte Werke*. Barth, J.A., Leipzig, 1895.
- [9] A.P. Christoforou and A.S. Yigit. Transient response of a composite beam subject to elasto-plastic impact. *Composites Engineering*, 5(5):459–470, 1995.
- [10] A. Henriksson. Transverse compressive behaviour of carbon-epoxy laminates and its influence on contact laws. Master's thesis, The Aeronautical Research Institute of Sweden, Stockholm, November 1990.
- [11] C.S. Lopes. *Damage and Failure of Non-Conventional Composite Laminates*. Phd thesis, Delft University of Technology, June 2009.
- [12] R.J.C. Creemers. Effect of impact damage and subsequent fatigue loading on thick composite structures: test results - vol 1. techreport NLR-CR-2011-437-VOL-1, NLR - Netherlands Aerospace Centre, 2011.